Title	Silver nanowire array-polymer composite as thermal interface material
Authors	Xu, Ju;Munari, Alessio;Dalton, Eric;Mathewson, Alan;Razeeb, Kafil M.
Publication date	2009
Original Citation	Xu, J., Munari, A., Dalton, E., Mathewson, A. and Razeeb, K. M. (2009) 'Silver nanowire array-polymer composite as thermal interface material', Journal of Applied Physics, 106(12), 124310 (7pp). doi: 10.1063/1.3271149
Type of publication	Article (peer-reviewed)
Link to publisher's version	http://aip.scitation.org/doi/10.1063/1.3271149 - 10.1063/1.3271149
Rights	© 2009, American Institute of Physics. This article may be downloaded for personal use only. Any other use requires prior permission of the author and AIP Publishing. The following article appeared in Xu, J., Munari, A., Dalton, E., Mathewson, A. and Razeeb, K. M. (2009) 'Silver nanowire array-polymer composite as thermal interface material', Journal of Applied Physics, 106(12), 124310 (7pp). doi: 10.1063/1.3271149 and may be found at http://aip.scitation.org/doi/10.1063/1.3271149
Download date	2024-04-24 07:18:30
Item downloaded from	https://hdl.handle.net/10468/4748

Silver nanowire array-polymer composite as thermal interface material

Ju Xu, Alessio Munari, Eric Dalton, Alan Mathewson, and Kafil M. Razeeb'

Citation: Journal of Applied Physics **106**, 124310 (2009); doi: 10.1063/1.3271149
View online: http://dx.doi.org/10.1063/1.3271149
View Table of Contents: http://aip.scitation.org/toc/jap/106/12
Published by the American Institute of Physics

Silver nanowire array-polymer composite as thermal interface material

Ju Xu,[1] Alessio Munari,[2] Eric Dalton,[2] Alan Mathewson,[1] and Kafil M. Razeeb[1,a)]
[1]*Tyndall National Institute, University College Cork, Lee Maltings, Cork, Ireland*
[2]*CTVR, Stokes Institute, University of Limerick, Ireland*

(Received 26 August 2009; accepted 8 November 2009; published online 22 December 2009)

Silver nanowire arrays embedded inside polycarbonate templates are investigated as a viable thermal interface material for electronic cooling applications. The composite shows an average thermal diffusivity value of 1.89×10^{-5} m^2 s^{-1}, which resulted in an intrinsic thermal conductivity of 30.3 W m^{-1} K^{-1}. The nanowires' protrusion from the film surface enables it to conform to the surface roughness to make a better thermal contact. This resulted in a 61% reduction in thermal impedance when compared with blank polymer. An ~30 nm Au film on the top of the composite was found to act as a heat spreader, reducing the thermal impedance further by 35%. A contact impedance model was employed to compare the contact impedance of aligned silver nanowire-polymer composites with that of aligned carbon nanotubes, which showed that the Young's modulus of the composite is the defining factor in the overall thermal impedance of these composites. © *2009 American Institute of Physics*. [doi:10.1063/1.3271149]

I. INTRODUCTION

As semiconductor device feature sizes continue to be reduced, ensuring reliable operation has become a growing challenge. The effective transfer of heat from an integrated circuit (IC) and its heat spreader to a heat sink is a vital step in meeting this challenge.[1] Microscopic surface roughness and nonplanarity of the IC/heat spreader and heat sink surfaces result in asperities between the two mating surfaces, which prevent the two solids from forming a thermally perfect contact due to the poor thermal conductivity of air that exists in the gaps between the two surfaces.[2] Thermal interface materials (TIMs) are, therefore, used to provide an effective heat conduction path between the two solid surfaces owing to their conformation to surface roughness and high thermal conductivity.[3] Different TIMs such as metallic foils, grease, phase change materials, adhesives, elastomer, and thermoplastic polymers have already been deployed for reducing the thermal impedance between joints.[4] The thermal impedance of this system is comprised of the combined thermal contact impedances of the two surfaces and the bulk thermal impedance of the TIM material. Elastomer and thermoplastic polymer TIM composites made of a low modulus polymer matrix and high thermally conductive particle fillers are already widely used. The typical thermal impedance between joints is above 1.0 °C cm^2 W^{-1} when using traditional particle-laden elastomeric pads.[5] However, TIMs with lower thermal impedance are required according to the 2007 ITRS roadmap.[6] Recently, advanced thermal management schemes using carbon nanotubes (CNTs) as filler particles in polymer or CNT arrays directly as TIMs have been suggested as a means to dissipate high heat fluxes while maintaining low chip temperatures. These proposals have been made on the basis of the high intrinsic thermal conductivity of CNTs.[7] So far, the reported effective thermal conductivity of CNT arrays range from 74 to 83 W m^{-1} K^{-1}, and the lowest thermal impedance between substrates obtained by using CNT array based TIMs is about 0.1 °C cm^2 W^{-1}, which is an order of magnitude lower than the commercial elastomeric pad TIMs.[8] However, while using the CNT arrays as TIMs has the potential to compete with state-of-art thermal pads, the fabrication of these CNT array thermal interfaces requires high temperature (above 700 °C) processes and these are incompatible with the temperature-sensitive substrates used in most semiconductor technologies. Furthermore, the electrical performance of most metal contacts and interconnects degrades when exposed to a temperature in excess of 450 °C for more than a very limited time.[8] Using *insertable* CNT array as a TIM has also been reported. However, in this case the contact impedance between the CNTs and substrates was found to be high. This was associated with nonuniform growth of CNTs preventing all of the CNTs in the film from making proper thermal contact to the opposing surface. Furthermore, the high Young's modulus of CNTs [0.8–0.9 TPa for multiwall CNTs, 1–5 TPa for single-wall CNTs[9]] prevents the array from conforming between surfaces and achieving good thermal contact.[8,10] The possibility of inadvertently incorporating contaminating impurities, the existence of voids between CNTs, and the growth conditions of CNT arrays greatly affect the effective thermal conductivity of CNTs, typically resulting in a TIM with a large performance uncertainty. In addition, the need for mass production due to the high commercial volumes requirement and the high cost of fabrication may be another hindrance to the industrial acceptance of this solution.

In this paper, we investigate a polymer composite that uses silver nanowire (AgNW) arrays—as opposed to CNT array—in a TIM. These nanowires have an average diameter of 220 nm and an aspect ratio of >100. Bulk silver has an excellent thermal conductivity of 429 W m^{-1} K^{-1} and it has a Young's modulus of 83 GPa, which is far lower than that of CNTs (800 GPa). This suggests a better conformability to the rough surface of the substrates and may permit achievement of superior thermal impedance than CNT-based TIMs. Fur-

a)Electronic mail: kafil.mahmood@tyndall.ie.

thermore, compared with the Ag particles/flakes that have already been widely used as fillers for many polymeric TIMs, the AgNW arrays are expected to be better effective thermal conduits due to their inherent continuity, vertically aligned orientation, and their ability to conform to micron-scale unevenness of the mating surfaces. Nanoporous polymer template can be used to fabricate these high aspect ratio nanowires by the electrodeposition techniques. However, thermal conductivity and, particularly, thermal impedance of these AgNW-polymer composites have not yet been reported. Furthermore, a comparison of aligned AgNW-polymer and CNT-polymer TIMs is necessary in order to understand the thermal contact impedance behavior of these two composites. As discussed above, thermal contact impedance characteristics are the performance defining parameter for any TIM.

II. EXPERIMENTAL

A. Sample fabrication and material characterization

The AgNW-polymer composite was fabricated by electrodeposition using a porous polycarbonate (PC) film (Millipore, pore density: ~20%, pore diameter: ~220 nm) as a template. Typically, a 100 nm Ag thin film was deposited at the bottom of the template to act as a seed and conductive layer. A bath comprising 50 g l^{-1} $AgNO_3$ and 200 g l^{-1} CH_3COONH_4 was prepared. De-ionized water with resistivity of ~18 MΩ was used to prepare the solution. Electrodeposition was performed with stirring at a constant 500 rpm. A current density of 1.0 mA cm^{-2} was applied and all the deposition was performed at room temperature. After deposition, the samples were thoroughly rinsed with de-ionized water, any Ag overgrowth was removed manually and dried with a nitrogen gun. After thermal impedance measurements of the as prepared samples, the top surface of the samples was coated with a 30 nm Au film by e-beam evaporation. This was to investigate the influence of a conductive metal layer on overall thermal impedance of the nanocomposite material. The top surface and the cross-sectional view of the AgNWs within the PC matrix were characterized by scanning electron microscopy (SEM) using a JOEL 200 SEM. For an estimation of overall grain size and crystal orientation, x-ray diffraction (XRD) measurements were carried out using a Philips PW3710 diffractometer with Cu $K\alpha_1$ radiation that had a wavelength of 1.540 598 Å.

B. Thermal diffusivity measurements

Thermal diffusivity measurement of the AgNW-PC composites was carried out using the laser flash method.[3,11] A short laser pulse (using Nd:yttrium aluminum garnet laser) of duration 7 ns was applied to the samples to create an effectively instantaneous heat source. The Ag seed layer side was heated with the laser pulse where the diameter of the laser beam was 4 mm. An infrared detector was positioned on the opposite side of the sample to where the pulse impinged in order to measure the thermal response that is generated during this illumination. The resulting rise in temperature was recorded using the preamplifier and oscilloscope setup, which was controlled using a LABVIEW program. In this method, heat flow is assumed to be one dimensional in the direction perpendicular to the planar surfaces. The duration of the pulse is short enough to be considered effectively instantaneous in comparison to the time taken for the thermal response to reach half of its maximum value. The time at which the curve reaches that value is given by the following equation:

$$t_{0.5} = \frac{1.38l^2}{\pi^2 \alpha}, \tag{1}$$

where α is the thermal diffusivity, l is the thickness of the sample, and $t_{0.5}$ is the time at which the thermal response at the opposite side of the sample reaches half of its maximum value. Diffusivity is calculated from the time $t_{0.5}$ and the thickness of the samples. All the measurements were conducted in air and therefore heat loss correction for radiative and convective heat losses was done according to Cowan.[12]

C. Thermal impedance measurements

To measure the thermal impedance of the composites, a modified ASTM D5470-06 standard setup was employed.[13,14] A detailed drawing of the experimental setup can be seen in Fig. 1(a), where different components are numbered to describe the setup. The meter bars (7) are made of two round copper C11600 rods 60 mm long and 20 mm diameter and have a nominal thermal conductivity of 388 W m^{-1} K^{-1} at 25 °C. The contact surfaces were ground with a Buehler grinder apparatus and polished with 1 μm diamond paste to get a mirror finish. The surface roughness was measured with an NT-MDT model atomic force microscope. Figures 1(c) and 1(d) show the representative topographic and the three-dimensional (3D) topographic images of the surface of copper calorimeter, which showed a root-mean-square (rms) roughness of 88 nm. Eight 0.5 mm diameter thermistors were embedded within the bars to measure the thermal gradients with an accuracy of ±0.01 °C between 0 and 70 °C. Calibration of the thermistors was performed with a Hart Scientific 5611T model reference probe with an absolute calibrated uncertainty of 0.002 °C. The thermistor resistances were recorded using two National Instruments DAQ-mx USB cards, each equipped with four channels and each in four-wire resistance configuration using a built-in low excitation current. Cooling of the lower meter bar was provided by a Lauda thermal bath constant-temperature cooler loop whose stability was ±0.02 °C. The upper meter bar was heated using an aluminum heater block with two internal 250 W cartridge heaters controlled by a Red-Lion PID controller. The heater block was attached to an AST KAF-S load cell with rated load of 2 kN ±0.2% (11). The load cell, in turn, was then attached to Nanotec ball screw linear actuator, which can apply a maximum force of 1.8 kN onto a surface of 3.14×10^{-4} m^2. Furthermore the actuator has a minimum step size of 1 μm resolution (15). The distance between the two mating surfaces of the bars was measured using an MX-Metralight laser micrometer with a 0.4 μm resolution (10), and thereby the bond line thickness (BLT) of the sample could be measured *in situ*. During testing, the meter bars were wrapped in an insulating material

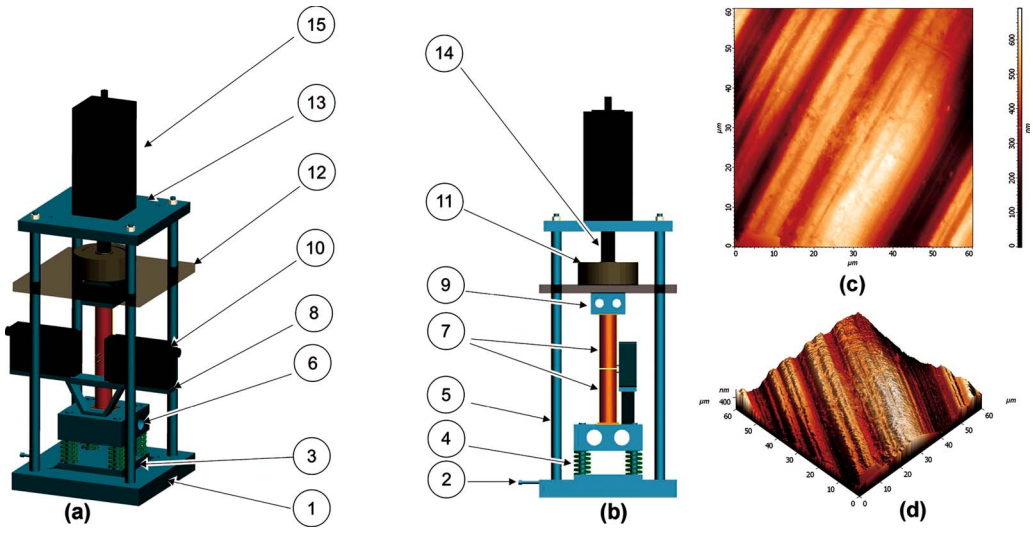

FIG. 1. (Color online) Cad design of the experimental apparatus. (a) Front view and (b) side view of the apparatus: (1) aluminum plate, (2) fine threaded linear screw for x-y displacement, (3) insulating Perspex plate, (4) compression springs, (5) aluminum shafts, (6) aluminum cooler block, (8) micrometer stand, (12) Perspex plate, (13) steel plates, and (14) stainless steel ball screw. (c) and (d) show the representative topographic and the 3D topographic images of the surface of copper calorimeter.

(not shown in Fig. 1) to minimize heat losses.

Calibration of the test facility was carried out by machining four stainless steel (303 grade) disks with different thicknesses. According to data sheets provided by the manufacturer, a nominal thermal conductivity of 15.10 W m^{-1} K^{-1} is expected at 29.27 °C, which is the mean temperature of the sample under test. Prior to testing, a thin layer of highly conductive thermal paste was spread onto both faces of the disk in order to minimize contact impedance as much as possible, because this differs from sample to sample depending on surface roughness. Each disk was compressed between the meter bars under a constant contact pressure of 1 MPa and the thermal impedance of the disk was measured. These measurements are plotted in Fig. 2 against their respective thicknesses. A linear fit is used for this set of data and the slope is equal to the inverse of the thermal conductivity of the bulk material. The effective thermal conductivity according to this simple calculation is found to be 15.01 W m^{-1} K^{-1}, which is within 0.59% of the manufacture's value of 15.10 W m^{-1} K^{-1}.

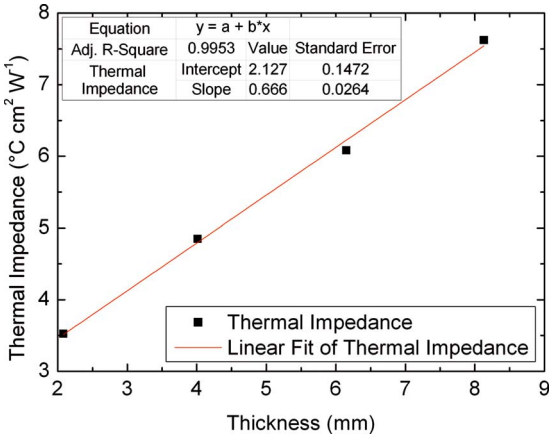

FIG. 2. (Color online) Measured thermal impedance vs thickness of 303 stainless steel disks.

III. RESULTS AND DISCUSSION

The SEM images of Fig. 3 indicate that the *as-grown* Ag arrays are vertically aligned. The top view of the nanocomposite film shows that AgNWs have extruded outside the PC membrane. It should be noted that the wires were distorted while preparing the sample for cross section analysis, as shown in the inset of Fig. 3(a). The nanometer size of these AgNW tips is expected to be able to conform to the submicron roughness of the substrate surfaces. Figure 3(b) shows the high magnification image of the top surface where the grains of the AgNW are visible.

The real filling ratio (ϕ) of AgNW within the PC membrane was calculated according to the following formula:

$$\phi = \frac{V_{Ag}}{V_T} = \frac{(W_2 - W_1)/\rho_{Ag}}{\pi D^2 h/4}, \tag{2}$$

where V_{Ag} is the volume of AgNW, V_T is the total volume of the PC membrane which includes unfilled pores, W_1 is the weight before deposition and W_2 is the weight of the sample after the Ag plating process, ρ_{Ag} is the density of silver, D is the diameter of deposited area, and h is the thickness of the membrane. A filling ratio of 9 vol % AgNW was obtained for the samples studied in this work.

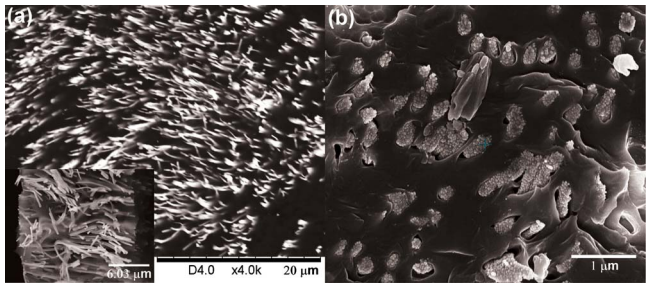

FIG. 3. (Color online) SEM images of AgNW arrays within PC matrix. (a) Top surface showing nanowires coming out of pores. The inset showing cross section, (b) top view.

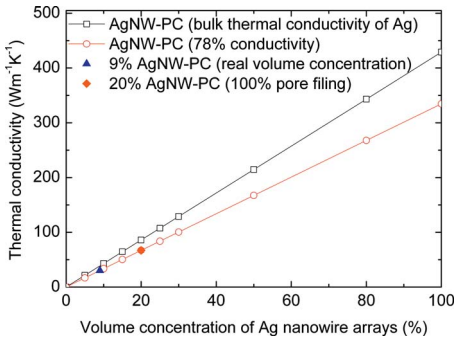

FIG. 4. (Color online) Thermal conductivity of AgNW-PC nanocomposite as a function of vol % of Ag.

According to the rule of mixtures for a simple parallel model, the effective thermal conductivity in the z direction is[3]

$$k_z = k_m(1-\phi) + k_p\phi, \tag{3}$$

where k_z is the thermal conductivity of the composite material along the z direction, i.e., perpendicular to the sample surface, k_m and k_p are the bulk thermal conductivities of the matrix and the AgNW, respectively, and ϕ is the volume percentage of the AgNW in the composite. Considering that the bulk thermal conductivity of PC is 0.2 W m^{-1} K^{-1} and Ag is 429 W m^{-1} K^{-1}, the calculated thermal conductivity of this composite is shown in Fig. 4 as a function of volume concentration of AgNW. The porosity of PC membrane is ~20%. Therefore, in case of 100% pore filling, the volume percentage of AgNW will be 20% in the polymer matrix. The calculated thermal conductivity value of this AgNW-PC composite is ~86 W m^{-1} K^{-1}, which is comparable to CNT arrays (74–83 W m^{-1} K^{-1}).

The thermal conductivity of the AgNW-PC composite was determined from the thermal diffusivity values, measured using the laser flash method described in Sec. II B and other works.[3] Figure 5 shows the thermograms of silver foil (purity of 99.99%, thickness of 265 μm), PC template (with a thickness of 24 ± 1 μm), before Ag nanowire formation (PC without AgNW) and after fabrication of AgNW-PC (thickness of 24 μm). The blank PC membrane with Ag seed layer on one side resulted in a thermal diffusivity of 0.0152×10^{-5} m^2 s^{-1} and pure Ag foil (265 μm thickness) showed a diffusivity value of 17.356×10^{-5} m^2 s^{-1}. These

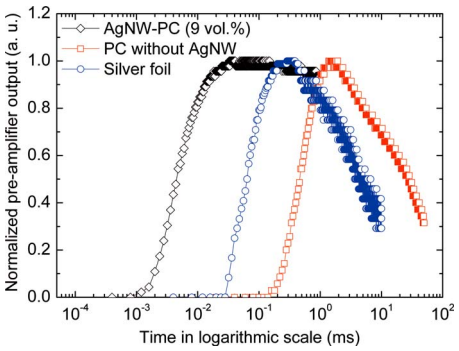

FIG. 5. (Color online) Thermal transients of AgNW-PC, PC template without AgNW, and silver foil.

values represent differences of 1.6% and 0.17%, respectively, when compared with values of PC and silver in the literature.[15] The values obtained for the composite varied from 1.82×10^{-5} to 1.96×10^{-5} m^2 s^{-1} and showed an average value of 1.89×10^{-5} m^2 s^{-1}. This shows a significant increase in the diffusivity of the composite to that of blank PC of a factor of 124.

Combining with the experimental thermal diffusivity value, Eq. (3) can be written as

$$k_{NC} = k_{PC}(1-\phi) + k_{Ag}\phi = \alpha[(\rho c)_{PC}(1-\phi) + (\rho c)_{Ag}\phi], \tag{4}$$

where k is the thermal conductivity and (ρc) is the heat capacity per unit volume. ϕ is the volume percentage of Ag in the composite and α is the thermal diffusivity of the composite. For 9% filling ratio of AgNW (as achieved in this paper), the calculated thermal conductivity is ~38.8 W m^{-1} K^{-1} according to Eq. (3). However, a thermal conductivity of 30.3 W m^{-1} K^{-1} was evaluated using Eq. (4) for the nanocomposite using the experimental diffusivity value and considering the density and the heat capacity of silver and PC. It is interesting to note that the calculated thermal conductivity value of the nanocomposite (k_{NC}) (38.8 W m^{-1} K^{-1}) using the modified effective medium theory overpredicted the experimental values when the bulk thermal conductivity of Ag was considered. However, when the thermal conductivity of Ag was reduced to ~78% of the bulk conductivity, the theoretical value showed excellent correspondence. In this case, AgNWs have an effective thermal conductivity of 334.6 W m^{-1} K^{-1}. In order to understand this conductivity reduction, an XRD analysis was carried out on AgNW samples. The XRD analysis revealed that the AgNWs are polycrystalline with a preferred orientation of (111). The Scherrer formula was employed to calculate the grain size of the AgNW, which showed an average grain size of 204 nm. A similar reduction in conductivity value for Ni nanowires has already been observed as an effect of grain size.[3] The deviation from bulk thermal conductivity in case of AgNW may be explained as follows: the thermal conduction in pure metals is usually dominated by electron rather than phonon conduction. Therefore, the thermal conductivity and diffusivity are dominated by the scattering process of conducting electrons. At room temperature, the electron mean free path of Ag is 52 nm.[16] Although the average grain size obtained from XRD measurements is four times the mean free path of the electron, it was reported that the grain size of electrodeposited AgNW could vary from ~10 to ~200 nm.[17] In electrodeposited AgNW, there are also large numbers of defects and dislocations in crystals and, therefore, the grain boundary scattering of conduction electrons is believed to be responsible for the reduction in measured thermal conductivity over the expected theoretical value.

In a publication by Huang *et al.*[18] it was shown that the electrical resistivity of a single crystalline trapezoidal AgNW is dominated by the electron diffusely scattering on the nanowire surface and explained their experimental results using Chamber's approach[19] to the Fuchs and Sondheimer theory.[20,21] Their work was focused to differentiate the sur-

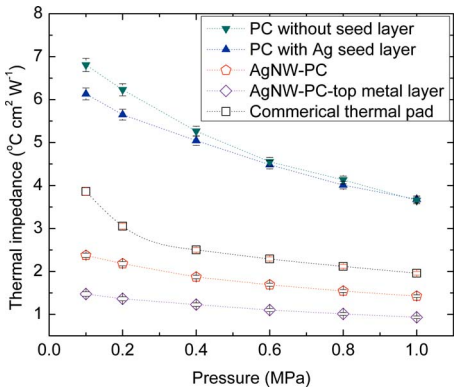

FIG. 6. (Color online) Thermal impedance (with error bars) of AgNW-PC composite and reference samples as a function of contact pressure.

face scattering from the grain boundary scattering and for single crystal wires the experimental resistivity fits well to the theoretical resistivity models that are close to purely diffuse surface scattering. Durkan *et al.*,[22] on the other hand, argued that in a polycrystalline wire, when the wire width is comparable to the average grain size, the grain boundary scattering is the dominant source of increased resistivity. Only when the wire width is below ~0.5 times the grain size, surface scattering becomes important and approaches to the same order of magnitude of grain boundary scattering. Similarly, it was observed that the surface scattering is intimately connected with the geometrical dimensions, i.e., diameter of the wires. This scattering becomes important when the diameter is comparable to or smaller than the mean free path of the conduction electrons of the respective metal.[23] In the present case, the nanowires are polycrystalline with an average grain size of ~204 nm and have a diameter of 220 nm, which is comparable to the grain size. Thereby, the grain boundary scattering will be the dominant factor in reducing the thermal diffusivity and conductivity of the AgNWs, rather than surface scattering.

The thermal impedances of the as-prepared AgNW-PC composite films with (AgNW-PC-top metal layer) and without the top metal layer (AgNW-PC) are shown in Fig. 6 as a function of applied contact pressure. To facilitate comparison, a blank PC template with a 100 nm Ag seed layer and a commercially available thermal pad is also included. The thermal impedance of the PC membrane before and after seed layer deposition did not show a large variation, specifically when the contact pressure exceeded 0.2 MPa. In the lower contact pressure range, the seed layer acted as a heat spreader and enhanced the heat transfer, which resulted in a further reduction in measured thermal impedance. However, as the contact pressure was increased, this effect diminished. The thermal impedance of the AgNW-PC composite sample showed at least a 61% reduction compared with the PC with seed layer under all measured contact pressures and a 29% reduction compared with commercial thermal pad. When a 30 nm Au film was deposited on top of the AgNW-PC film, the thermal impedance was reduced by another 35% to 0.93 °C cm^2 W^{-1} at a contact pressure of 1.0 MPa. The SEM analysis on different areas of the AgNW-PC samples revealed that not all of the nanowires came out of the pores due to nonhomogeneity in the pore structure. The deposited Au film effectively connected most of the nanowires together and thereby increased the effective contact area. As a result, the thermal impedance decreased, which was also reported for CNT arrays.[24,25] This limiting of contact area (without top metal layer) leads to an increase in the contact impedance, ultimately increasing the overall impedance of the TIM. The contribution of contact impedance will be explored in Sec. IV.

IV. CONTACT IMPEDANCE MODEL

The two most important parameters for a TIM are its thermal contact impedance and bulk conductivity. The following section employs a thermal impedance model[26] to explore how these two parameters affect the thermal impedance as a function of decreasing BLT for both aligned AgNW and aligned CNT embedded in a PC matrix. With decreasing BLT, the percentage contribution of the contact to overall thermal impedance increases and is of critical importance to the thermal behavior of an interface material. According to Singhal *et al.*,[26] the thermal contact impedance of two mating surface can be calculated from

$$R_c = \frac{1}{1.55}\left(\frac{\sigma}{\tan\theta}\right)\left[\frac{E_{\mathrm{NC}}\tan\theta}{\sqrt{2p}(1-v_e^2)}\right]^{0.94}\frac{1}{2}\left(\frac{1}{k_1}+\frac{1}{k_{\mathrm{NC}}}\right), \quad (5)$$

where p is the contact pressure, σ is the rms surface roughness, $\tan\theta$ is the average slope of the asperities of the two contact surfaces and is equal to $0.125\sigma^{0.402}$, k_1 and k_{NC} are the thermal conductivity of the mating surface and composite, respectively, v_e is the Poisson's ratio, and E_{NC} the Young's modulus of the composite. In this case, the mating surfaces are the composite's surface and the surface of a

TABLE I. Values used in contact impedance calculations.[15]

Materials	Young's modulus (Pa)	Poisson's ratio	Thermal conductivity (W m^{-1} k^{-1})
Copper calorimeter	117×10^9	0.37	388
Silver	83×10^9	0.37	429
PC	2.3×10^9	0.37	0.2
CNT	80×10^{10}	0.08	6000
Silver-PC composite	6.3×10^9	0.37	38.8 9 vol % of AgNW
CNT-PC composite	4.5×10^{10}	0.35	180 9 vol % of CNT

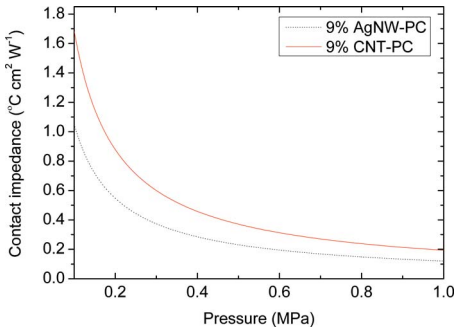

FIG. 7. (Color online) Contact impedance produced by 9 vol % loaded AgNW aligned in a PC matrix (9% AgNW-PC) and aligned 9 vol % loaded CNT in a PC matrix (9% CNT-PC) as a function of contact pressure with a fixed BLT of 30 μm.

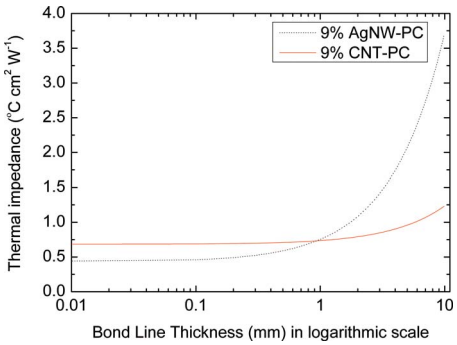

FIG. 8. (Color online) Thermal impedance produced by 9 vol % loaded AgNW aligned in a PC matrix (9% AgNW-PC) and aligned 9 vol % loaded CNT in a PC matrix (9% CNT-PC) as a function of BLT at a fixed contact pressure of 0.5 MPa.

copper calorimeter (used in the thermal impedance measurement) with a rms roughness of 88 nm.

A modified effective medium theory [Eq. (3)] is used to calculate the equivalent elastic modulus and effective Poisson's ratio of both the composites. The thermal conductivity of the CNT-PC composite is calculated by Eq. (6), developed by Nan *et al.*,[27]

$$k_e = \left(1 + \frac{fk_c}{3k_m}\right)k_m, \tag{6}$$

where k_e is the effective conductivity of the composite, k_c and k_m are the thermal conductivity of the CNT and matrix, respectively, and f is the fractional volume content of the CNTs. The effective thermal conductivity of the AgNW-PC is taken as 30.3 W m^{-1} K^{-1} from the thermal diffusivity measurements. It should be noted that for these calculations an intrinsic thermal conductivity of 6000 W m^{-1} K^{-1} is used for the CNTs. However it has been shown that an aligned CNT material has generally a far lower thermal conductivity value,[28] typically 3000 W m^{-1} K^{-1}. The parameters and the associated values used in the contact impedance model are shown in Table I.

As can be seen from Fig. 7, AgNW-PC has a significantly lower contact impedance than that of the aligned CNT-PC for all contact pressure ranges up to 1 MPa. Although there is an increase in the thermal conductivity of the PC matrix by the introduction of the CNTs, the increase in the contact impedance due to the stiffening of the composite essentially diminishes much of the gain. Since the Young's modulus of the silver used in the PC is an order of magnitude lower than that of CNTs, AgNW-PC composite does not suffer from this problem to the same extent. It was also observed that if the BLT of the material is increased, the contact impedance becomes less of a concern in the overall (total) thermal impedance of the composite. This is shown in Fig. 8 (at a set contact pressure of 0.5 MPa) and, as would be expected, the CNT-PC composite surpasses the AgNW composite at the larger BLT, in this case at 0.95 mm. This is essentially showing that for thinner TIM, the most important aspect is the Young's modulus and not the intrinsic thermal conductivity.

V. CONCLUSIONS

In summary, we have fabricated AgNW-PC composites and examined their properties as TIMs. The protrusion of nanowires from the polymer film surface enables it to conform to surface roughness and this results in a reduction in thermal impedance of 61% when compared to a blank template. A thin Au film on the top of the composite was found to act as a heat spreader, which further reduced the thermal impedance value by 35%. With emphasis on the contact impedance influence on the overall thermal impedance, it is shown through the contact impedance model that for any TIM, when there is a decrease in the thickness, the Young's modulus becomes the dominant factor as opposed to its intrinsic thermal conductivity.

ACKNOWLEDGMENTS

This work is financially supported by Enterprise Ireland under commercialization fund technology development program (Grant No. CFTD/2008/322) and Science Foundation Ireland under CTVR program (Grant No. 03/CE3/I405).

[1] B. A. Cola, P. B. Amama, X. F. Xu, and T. S. Fisher, ASME Trans. J. Heat Transfer **130**, 114503 (2008).
[2] R. S. Prasher, P. Koning, J. Shipley, and A. Devpura, J. Electron. Packag. **125**, 386 (2003).
[3] K. M. Razeeb and S. Roy, J. Appl. Phys. **103**, 084302 (2008).
[4] I. Savija, J. R. Culham, M. M. Yovanovich, and E. E. Marotta, J. Thermophys. Heat Transfer **17**, 43 (2003).
[5] R. Viswanath, V. Wakharkar, A. Watwe, and V. Lebonheur, Intel Technol. J. **4**, 16 (2000).
[6] http://www.itrs.net/links/2007itrs/2007_chapters/2007_assembly.pdf,
[7] R. Prasher, Proc. IEEE **94**, 1571 (2006).
[8] B. A. Cola, X. F. Xu, and T. S. Fisher, Appl. Phys. Lett. **90**, 093513 (2007).
[9] D. Srivastava, C. Wei, and K. Cho, Appl. Mech. Rev. **56**, 215 (2003).
[10] P. K. Schelling, L. Shi, and K. E. Goodson, Mater. Today **8**, 30 (2005).
[11] W. J. Parker, R. Jenkins, C. P. Butler, and G. L. Abbot, J. Appl. Phys. **32**, 1679 (1961).
[12] R. D. Cowan, J. Appl. Phys. **34**, 926 (1963).
[13] K. M. Razeeb, A. Munari, E. Dalton, J. Punch, and S. Roy, *2007 ASME-JSME Thermal Engineering Conference and Summer Heat Transfer Conference* (ASME, Vancouver, BC, 2007), pp. 817–823.
[14] A. Munari, J. Xu, E. Dalton, A. Mathewson, and K. M. Razeeb, *2009 Electronic Components and Technology Conference* (IEEE, San Diego, CA, 2009), pp. 448–452.
[15] *CRC Handbook of Chemistry and Physics*, edited by R. C. Weast (CRC, Florida, 1994).
[16] W. Zhang, S. H. Brongersma, O. Richard, B. Brijs, R. Palmans, L. Froyen,

and K. Maex, Microelectron. Eng. **76**, 146 (2004).
[17]I. Kazeminezhad, A. C. Barnes, J. D. Holbrey, K. R. Seddon, and W. Schwarzacher, Appl. Phys. A: Mater. Sci. Process. **86**, 373 (2007).
[18]Q. Huang, C. M. Lilley, and M. Bode, Appl. Phys. Lett. **95**, 103112 (2009).
[19]R. G. Chambers, Proc. R. Soc. London, Ser. A **202**, 378 (1950).
[20]K. Fuchs, Proc. Cambridge Philos. Soc. **34**, 100 (1938).
[21]E. H. Sondheimer, Adv. Phys. **1**, 1 (1952).
[22]C. Durkan and M. E. Welland, Phys. Rev. B **61**, 14215 (2000).
[23]W. Steinhögl, G. Schindler, G. Steinlesberger, and M. Engelhardt, Phys. Rev. B **66**, 075414 (2002).
[24]Y. Wu, C. H. Liu, H. Huang, and S. S. Fan, Appl. Phys. Lett. **87**, 213108 (2005).
[25]M. A. Panzer, G. Zhang, D. Mann, X. Hu, E. Pop, H. Dai, and K. E. Goodson, ASME Trans. J. Heat Transfer **130**, 052401 (2008).
[26]V. Singhal, T. Siegmund, and S. V. Garimella, IEEE Trans. Compon. Packag. Technol. **27**, 244 (2004).
[27]C. W. Nan, Z. Shi, and Y. Lin, Chem. Phys. Lett. **375**, 666 (2003).
[28]Y. Gogotsi, *Nanomaterials Hbk.* (CRC, Florida/Taylor & Francis, London, 2006).